Molecular basis of the anticancer, apoptotic and antibacterial activities of Bombyx mori Cecropin A

Francisco Ramos-Martín, Claudia Herrera-León, Nicola d'Amelio

Molecular basis of the anticancer, apoptotic and antibacterial activities of *Bombyx mori* Cecropin A

Francisco Ramos-Martín[1,*], Claudia Herrera Léon[1] and Nicola D'Amelio[1,*]

[1] Unité de Génie Enzymatique et Cellulaire UMR 7025 CNRS, Université de Picardie Jules Verne, Amiens, 80039, France

* To whom correspondence should be addressed. Tel: +33 3 22 82 7473; Fax: +33 3 22 82 75 95; Email: nicola.damelio@u-picardie.fr. Correspondence may also be addressed to francisco.ramos@u-picardie.fr.

Highlights

- CecA is one of the few AMPs with *in-vitro* and *in-vivo* activity against esophageal cancer.
- The mechanism by which CecA selectively recognises and kills cancer cells is unknown.
- We show how CecA selectively targets cancer and mitochondrial biomimetic membranes.
- The formation of a three helical bundle helps CecA adapt to its target membranes.
- By NMR and MD we propose a mechanism for the induction of apoptosis in cancer cells.

Conflicts of interest: The authors declare that they have no competing interests.

Abstract: As Cecropin XJ, Cecropin A from *Bombyx mori* is one of the very few antimicrobial peptides having shown activity against esophageal cancer cells. It displays remarkable sequence-similarity to Cecropin XJ but slightly enhanced activity. In this work we show by NMR that both peptides are unstructured in solution but get structured in the presence of DPC micelles, mimicking the surface of biological membranes. In order to get insight into the molecular basis of its anticancer, antimicrobial and antifungal activity, we have investigated by MD simulations their interaction with a large variety of lipid bilayers mimicking cancer, mitochondrial, bacterial and fungal membranes. At variance with CecXJ, organized in two main helices, CecA tends to form a three helix bundle resulting in enhanced adaptability to its membrane targets. A specificity for the headgroup of phosphatidylserine and affinity for phosphatidylglycerol and cardiolipin may account for its selective targeting of cancer, bacterial and mitochondrial membranes, respectively.

Keywords: antimicrobial peptide, anticancer, esophageal carcinoma, antibiotic resistance, NMR, molecular dynamics

Abbreviations:

AMPs: antimicrobial peptides; DPC: Dodecylphosphocholine; NMP: N-methyl-2-pyrrolidone; HBTU: 2-(1H-benzotriazol-1-yl)-1,1,3,3-tetramethyluronium hexafluorophosphate; DIEA: N,N-diisopropylethylamine; TFA: trifluoroacetic acid; PE: phosphatidylethanolamine; PG: phosphatidylglycerol; PI: phosphatidylinositol; PS: phosphatidylserine; CL: cardiolipin; NPT: isothermal-isobaric ensemble ; LINCS: LINear Constraint Solver; PBC: Periodic Boundary Conditions; PME: particle mesh Ewald; RMSD: root-mean-square deviation; TSP-d4: Deuterated sodium 3-(trimethylsilyl)propionate-d4; DPC: dodecylphosphocholine; POPC: 1-palmitoyl-2-oleoyl-glycero-3-phosphocholine; POPG: 1-palmitoyl-2-oleoyl-sn-glycero-3-phospho-(1'-rac-glycerol); POPS: 1-palmitoyl-2-oleoyl-sn-glycero-3-phospho-L-serine; POPE: 1-palmitoyl-2-oleoyl-sn-glycero-3-phosphoethanolamine; POPI: 1-palmitoyl-2-oleoyl-sn-glycero-3-phosphoinositol; CSI: Chemical Shift Index; CHO: cholesterol.

1. Introduction

Esophageal cancer (EC) is an aggressive lethal malignancy representing major public health concerns worldwide. Its fast progression and late diagnosis lead to poor prognosis and high mortality [1], making it the sixth most common cause of cancer death in the world [2]. It is classified into two main histopathological subtypes: esophageal squamous cell carcinoma (ESCC) and esophageal adenocarcinoma (EAC). Despite important differences in cellular origin, incidence, epidemiology, and molecular signatures, both share poor outcomes with low 5-year overall survival rate [2]. The incidence increases with age and EAC is on average acquired around ten years earlier than ESCC. Most importantly, it is the solid malignancy with the fastest rise in incidence of the last four decades [1,2]. Gastroesophageal reflux is the most documented risk factor for EAC, which can gradually evolve from the premalignant Barrett's esophagus [1]. Recent improvements of oncological protocols and surgical management have failed to improve patient outcomes. Current treatments are heterogeneous in their mode of action and based in alkylating agents or antimetabolites which cause severe side effects, including antimicrobial resistance [3]. The use of chemotherapeutic agents often leads to drug resistance in EC patients [4]. The observed multidrug resistance (MDR) involves an increase in drug efflux, a decrease in drug influx, activation of DNA repair mechanisms, among other

mechanisms [4,5]. Recurrences are still a major problem, while only a few new targeted agents have been approved (trastuzumab and ramucirumab) [6–8].

In this scenario, it is clear that new approaches are urgently needed, improving the therapeutic outcomes of EC patients. Anticancer peptides (ACPs), which can be considered as a subclass of antimicrobial peptides (AMPs), are receiving increasing attention [9] for their ability to selectively kill cancer cells by inducing their lysis. These peptides act via a non-receptor-mediated pathway against the target cell membranes. Differences in charge and fluidity between the plasma membranes of most human cells and that of cancer cells, drive ACPs to their targets, accounting for their selectivity and low toxicity. The presence of sialic-acid-rich glycoproteins, heparan sulfate or phosphatidylserine (PS) [10] (but also PE and PI phospholipids [11,12] in the case of EC) on the surface of cancer cells attracts positively charged ACPs. The binding of ACPs to cell membranes can prevent the action of growth factors or inhibit proteins involved in the progression of cancer (such as kinase/protease involved in tumor growth, invasion, and metastasis) or block angiogenesis [5,13]. By binding to transporters (e.g. ABC family), they can even reverse resistance phenomena [5,13]. The mode of action of most AMPs makes them less prone to the development of resistance [5,13] because of the difficulty to change the lipidic organization of membranes by a simple point mutation, their fast killing rate [14] and because transfer of AMP resistance genes is infrequent[15]. Finally, AMPs can in some cases act by modulating the immune response, stimulating natural killer lymphocytes, and induce the production of interferon [13].

A particular class of ACPs are mitochondrial penetrating peptides (MPPs), able to trigger apoptosis via mitochondrial membrane disruption [16]. They can also be considered cell penetrating peptides (CPPs) because of their ability to penetrate the cell without damaging the plasma membrane [9]. The exact mechanisms by which these peptides enter the cells remain poorly understood, but their translocation does not necessarily involve an energy-dependent endocytic process [17]. In some cases, ACPs bind to PS exposed on the external leaflet of target membranes by means of arginine residues, and penetration relies on phospholipid flip-flop phenomena or other translocating mechanisms [17–20]. In mitochondria, the absence of drug degrading enzymes and DNA repairing systems [21,22] fixing the damage caused by grafted drugs [21,22] accounts for the reduced tendency to resistance of MPPs. Furthermore, the mitochondrion offers drugs a special protection from the

action of efflux pumps [23]. For MPPs, additional selectivity can be provided by the presence of cardiolipin (CL) in the mitochondrial membrane and a peculiar membrane potential [24].

Being a subclass of AMPs, many ACPs also possess antibacterial properties. The specificity of the biological action depends on the phospholipid composition of the plasma membrane which is different among bacterial species, cancer cells and mitochondria. Interestingly, common traits are found between bacteria and mitochondria (such as the presence of cardiolipin), accounting for the co-existence of apoptotic and antibacterial properties in MPPs [25].

Until now, only few AMPs have been described with activity against EC, all produced by *Bombyx mori*: Cecropin XJ (CecXJ) [26,27], Cecropin A (CecA) and Cecropin D (CecD) [28]. *Bombyx mori* CecropinA is an AMP composed of 37 amino acids with sequence RWKLFKKIEKVGRNVRDGLIKAGPAIAVIGQAKSLGK. Its anticancer activity has been shown with leukemia [28,29], esophageal Eca109 and TE13 cancer cells [28]. CecA was shown to inhibit proliferation, migration, invasion and even tumor growth *in-vivo* in a xenograft mouse model [28]. Besides its anticancer action, CecA analogs have shown immunomodulatory properties for the treatment of inflammatory diseases [30,31] and antimicrobial activity against *Acinetobacter baumannii*, *Pseudomonas aeruginosa*, *Escherichia coli* and *Agrobacterium*. In particular, CecA has shown activity against bacteria (*Klebsiella pneumoniae* and *Pseudomonas aeruginosa*) [32], fungi (*Botrytis cinerea* and *Fusarium* [33] and entomopathogenic fungus *Beauveria bassiana* [34]) and even HIV [32].

CecA is thought to inhibit EC cells by activating the mitochondria-dependent apoptotic pathway [28,35] after disruption of their membranes [28]. Despite the high potentiality, the details on its mechanism of action are still largely unknown [32] and a description at atomic level of the interaction of CecA with the membranes of cancer cells, bacteria, and mitochondria is needed for its development as an anticancer and antibacterial agent. In this work, we show by a combination of experimental and computational methods that CecA strongly interacts with biomimetic models of cancer membranes but selectively penetrate in mitochondrial membrane models, thus explaining its CPP and MPP properties. A detailed comparison with the sequence-related CecXJ (a member of the cecropin-B family) [16,36] is also provided, explaining why the substitution of key residues allow CecA to be more flexible and more easily adaptable to its membrane targets.

2. Material and methods

2.1. Molecular Dynamics Simulations

Systems for simulations were prepared using CHARMM-GUI [37]. A total of 128 lipid molecules were placed in each lipid bilayer (i.e., 64 lipids in each leaflet) and peptide molecules were placed over the upper leaflet at non-interacting distance (>10Å). Lysine and arginine residues were protonated. Initial peptide structure was obtained with PEP-FOLD3 [38]. Amidation of the C-terminus was achieved via the CHARMM terminal group patching functionality, integrated in CHARMM-GUI. For simulations with 8 peptides, the initial structure was obtained by placing each peptide next to the other avoiding close contacts. A water layer of 50-Å thickness was added above and below the lipid bilayer which resulted in about 15000 water molecules (30000 in the case of CL) with small variations depending on the nature of the membrane. Systems were neutralized with Na^+ or Cl^- counterions.

MD simulations were performed using GROMACS software [39] and CHARMM36m force field [40] under semi-isotropic (for bilayers) and isotropic (for micelles) NPT conditions. The TIP3P model [41] was used to describe water molecules. Each system was energy-minimized with a steepest-descent algorithm for 5000 steps. Systems were equilibrated with the Berendsen barostat [42] and Parrinello-Rahman barostat [43] was used to maintain pressure (1 bar) semi-isotropically with a time constant of 5 ps and a compressibility of 4.5×10^{-5} bar^{-1}. Nose-Hoover thermostat [44,45] was chosen to maintain the systems at 310 K with a time constant of 1 ps. All bonds were constrained using the LINear Constraint Solver (LINCS) algorithm, which allowed an integration step of 2 fs. PBC (Periodic Boundary Conditions) were employed for all simulations, and the particle mesh Ewald (PME) method was used for long-range electrostatic interactions. After the standard CHARMM-GUI minimization and equilibration steps [37], the production run was performed for 500 ns. The whole process (minimization, equilibration and production run) was repeated once in the absence of peptide and twice in its presence. Convergence was assessed using RMSD and polar contacts analysis.

All MD trajectories were analyzed using GROMACS tools and Fatslim [46]. Graphs and images were produced with GNUplot and PyMol [47].

2.2. *Synthesis of peptide*

CecA (RWKLFKKIEKVGRNVRDGLIKAGPAIAVIGQAKSLGK) and CecXJ (RWKIFKKIEKMGRNIRDGIVKAGPAIEVLGSAKAIGK) peptides were synthesized by GeneCust company (Boynes, France) and purity (>95%) was confirmed by analytical HPLC and MS. Both were amidated at their C terminus.

2.3. NMR Sample preparation, NMR experiments and analysis

For backbone resonance assignment, lyophilized samples of CecA and CecXJ were hydrated with 500 µl of 50 mM phosphate buffer pH 6.6 containing 10% of D_2O as a field-locking signal. The peptide final concentration was 0.8 mM or 1.6 mM. A set of 2D $^{1}H,^{13}C$-HSQC, $^{1}H,^{1}H$-TOCSY (mixing of 90 ms), and $^{1}H,^{1}H$-NOESY (mixing of 200 ms) were acquired at 278 K and 298 K on a Bruker 500 MHz UltraShield NMR spectrometer equipped with a BBI 5 mm probe. Deuterated sodium 3-(trimethylsilyl)propionate-d4 (TSP-d4) at a concentration of 100 µM was used as internal reference for chemical shift. NMR data was analyzed and processed using Bruker TopSpin 4 software.

For assignment and determination of secondary structure, a 0.8 mM sample of CecA was prepared as described above and then titrated with a 1 M stock solution of DPC:d38 to a final concentration of 100 mM. Titration was followed by 1D ^{1}H-NMR at 298 K. For the assignment of the interacting form of the peptide 2D $^{1}H,^{13}C$-HSQC, $^{1}H,^{1}H$-TOCSY (mixing of 60 ms), and $^{1}H,^{1}H$-NOESY (mixing of 200 ms) were recorded at a total DPC concentration of 100 mM. Reference random coil values in our experimental conditions (T = 278 K or 298 K, pH 6.6 and ionic strength 0.05 M) were calculated by POTENCI web server (https://st-protein02.chem.au.dk/potenci/) [48].

3. Results and discussion

3.1. The comparison with the sequence-related CecXJ highlights unique features of CecA

Net charge and hydrophobicity/amphipathicity are key features modulating AMP activities [49–52]. Both CecA and CecXJ are highly charged peptides (+8 and +9 respectively) which can form amphipathic alpha helices (compare helical wheels in Figure 3D). CecA displays a high sequence homology with CecXJ (Figure 1A), including the AGPA motif separating the sequence in two helices called helix I and II. Other common features include the amphipathic nature of helix I, the presence of aromatic residues at the N terminus and at least two lysine residues in both helices. An important difference resides in the substitution M11 with valine, a beta branched amino acid. Just like glycine

residues are known to weaken the helical conformation due to their flexibility, beta branched residues are considered helical breakers [53] because they increase the entropic cost of helix formation, due to the restricted motions of their side-chain in helical conformation [54,55]. In the case of CecA M11V substitution might break helix I into two.

Finally, the loss of E27 increases the positive charge of CecA and could possibly enhance its affinity to negatively charged membranes of cancer cells, mitochondria, bacteria and fungi.

3.2. MD simulations suggests the formation of a three helix bundle in CecA

Our MD simulations in solution confirm what was hypothesized by the comparison of CecXJ and CecA sequences. DSSP (Define secondary structure of proteins) [56] secondary structure prediction analysis clearly show (Figure 1B,C) that, while G12 alone in CecXJ is not able to destabilize helix I (Figure 1C) [36], the introduction of V11 contributes synergically to its destabilization and favours the formation of two fragments hereon called helix Ia and helix Ib (Figure 1B). Simulations also show that the two fragments are stabilized by salt bridges between the side chains of K6 and E9, R13 and D17, K21 and D17, which are also present in CecXJ [36].

The loss of E27 in CecA, which in CecXJ interacts with R1 stabilizing the U-shaped pairing of helix I and helix II [36], leads to a more complex network of interactions (Figures S1,S2). As a consequence of both factors, CecA is mostly found as a three helix bundle constituted by helix Ia, Ib and II and this is even more apparent in its interaction with membranes (see further in the text). Another consequence of the loss of E27 is an increased hydrophobicity of helix II, triggering a tendency to self-aggregation. Our simulations with multiple peptides clearly show the formation of dimers quickly evolving to higher order multimers (see Figure S3).

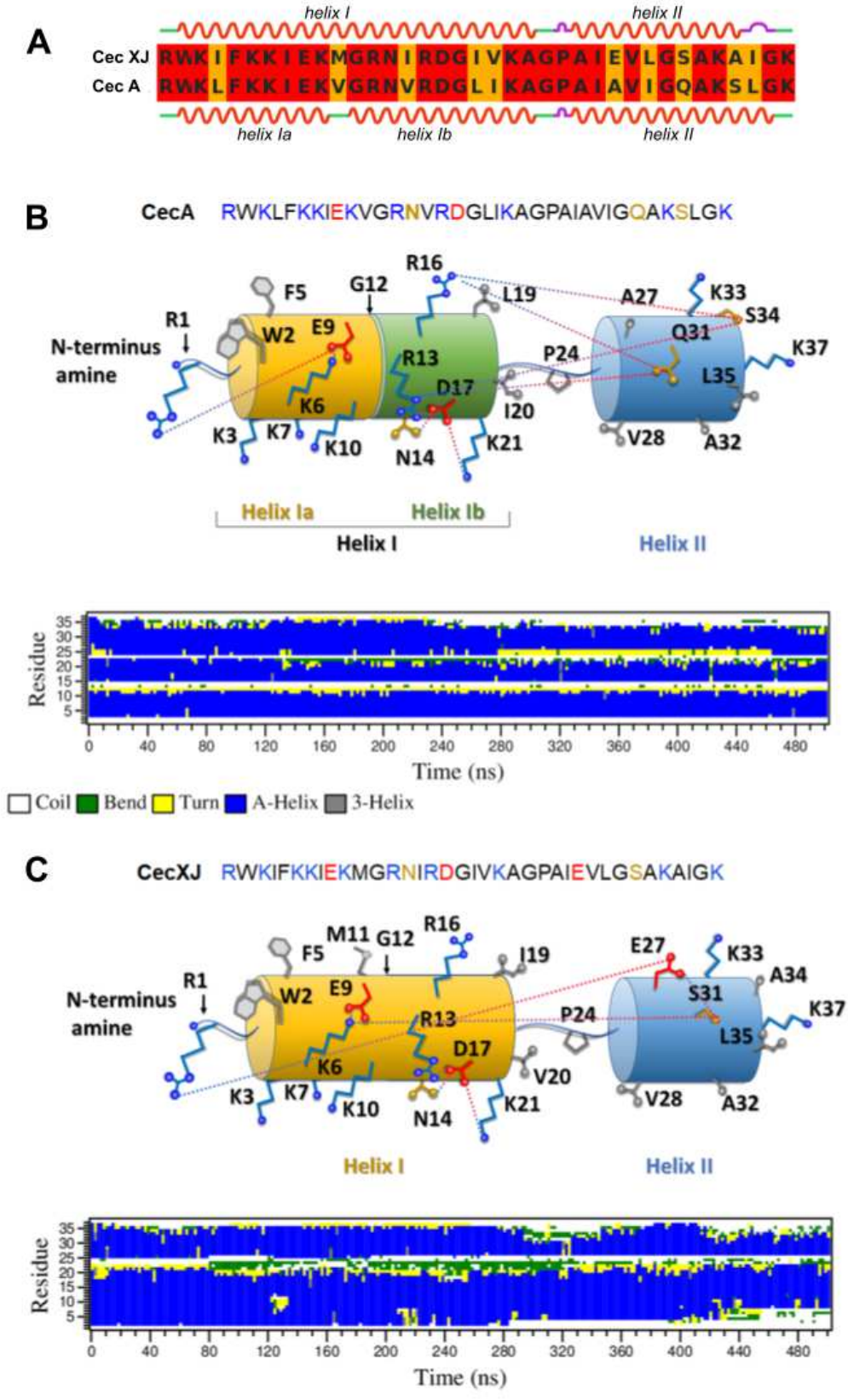
A
helix I
helix II
Cec XJ RWKIFKKIEKMGRNIRDGIVKAGPAIEVLGSAKAIGK
Cec A RWKLFKKIEKVGRNVRDGLIKAGPAIAVIGQAKSLGK
helix Ia
helix Ib
helix II
B
CecA RWKLFKKIEKVGRNVRDGLIKAGPAIAVIGQAKSLGK
N-terminus amine
R1
F5
G12
R16
L19
A27
K33
S34
K37
W2
E9
R13
P24
Q31
L35
K6
D17
I20
K3
K7
K10
N14
K21
V28
A32
Helix Ia
Helix Ib
Helix I
Helix II
Residue
Time (ns)
Coil
Bend
Turn
A-Helix
3-Helix
C
CecXJ RWKIFKKIEKMGRNIRDGIVKAGPAIEVLGSAKAIGK
N-terminus amine
R1
F5
M11
G12
R16
I19
E27
K33
A34
K37
W2
E9
R13
P24
S31
L35
K6
D17
V20
K3
K7
K10
N14
K21
V28
A32
Helix I
Helix II
Residue
Time (ns)

Figure 1. (A) *Sequence homology between CecXJ and CecA . Residues with 100 % homologies are coloured in red while those with a homology between 50 and 79 % are shown in orange. Homologies were calculated by ADAPTABLE web-server according to BLOSUM45 substitution matrix [57].* ***(B, C)*** *Schematic structure and elements of secondary structures along MD trajectories of CecA (**B**) and CecXJ (**C**). Hydrophobic amino acids are represented in gray, those with positive charge (K,R) in blue, negatively charged (D,E) in red and polar amino acids (N, S, Q) in yellow. Alpha-helical structures (helix I and helix II) are separated by the AGPA motif (residues 22-25), as shown in the DSSP diagram, and stabilized by salt bridges (dashed lines) between the side chains of K6 and E9, R13 and D17, K21 and D17. The replacement of M for V at position 11 in helix I results in a local loss of helical conformation in CecA, determining its tendency to fold in three helices.*

3.3. Solution state NMR experiments cast light on the structural features of CecA and CecXJ in solution and their interaction with DPC micelles

The behaviour of CecA and CecXJ in solution was studied by NMR spectroscopy to get insight into their structural differences.

3.3.1. CecA is unstructured in solution but gets structured in the presence of DPC micelles

Similarly to CecXJ, which was shown to be unstructured in solution [58] and assume alpha helical conformation in the presence of target membranes [36], CecA appears unstructured in solution according to our NMR data. Complete ^{1}H and ^{13}C backbone assignment (HN, H_{α} and C_{α}) of CecA in water was obtained by means of $^{1}H,^{1}H$-TOCSY, $^{1}H,^{1}H$-NOESY, and $^{1}H,^{13}C$-HSQC NMR experiments (Figure 2A and S4A,C). The comparison of chemical shift values with those expected for a random coil in the same experimental conditions, clearly show deviations under the significant threshold (0.1 ppm for ^{1}H and 0.7 ppm for ^{13}C [59]) (Figure 2C,D). Similar results were obtained for CecXJ (Figure 2B,E,F and S4B,D), thus confirming previous CD studies [58] but with single residue resolution.

In order to verify the hypothesis that CecA and CecXJ get structured upon interaction with their targets [36], we studied both peptides in the presence of DPC micelles, as a rough model of biological membranes. The ^{1}H spectrum of both peptides change dramatically when DPC micelles are added to their sample (Figure S5A). Peaks in the amide regions broaden beyond detection and re-

appear with an apparent larger linewidth at different frequencies, testifying a significant interaction in the semi-slow exchange regime in the NMR time scale (Figure S5A).

Despite the significantly large linewidth, the presence of alpha helical structure is confirmed by the appearance of HN/HN NOEs in the amide proton regions. Assignment of the peptide in the presence of DPC micelles was achieved for HN and H_α protons (H_α/C_α peaks disappear from the HSQC spectrum, probably due to severe transversal relaxation), whose negative deviations from random coil values allowed to monitor the formation of an alpha helix as shown in Figure 3A. The negative deviations expected for an alpha helix are interrupted at the level of E9-K10, D17-G18, K21 at the beginning of the loop separating helices I and II, and become somehow less pronounced starting from Q31 till the end of the sequence. Loss of local structure is often accompanied by higher mobility and a consequent reduction in the broadening of signal. Indeed, few peaks in the assigned region (HN/H_α region of NOESY spectrum in Figure S5B) display higher intensity than others and in particular the N-terminus (K3-L4; R1-W2 are not detectable probably due to exchange with the solvent), the central part of helix I (K10-V11), the loop interconnecting helices I and II (A22 and A25) and the C terminus (residues 31-37). While higher mobility in the loops and at the termini are common in proteins, more interesting is the mobility in the proximity of G12 which would confirm the weakening of the helix I hypothesized in section 3.1 and supported by MD simulations (Figure 1, 3B,C and S6).

3.3.2. CecXJ also gets structured in the presence of DPC micelles

In the case of CecXJ, spectra in the presence of DPC are very similar to those obtained for CecA but the broadening is more severe, preventing the assignment of most signals. However, H_α protons shift upfield, a phenomenon compatible with the formation of alpha helical structures [60]. The fragment at the center of the helix I (K10-M11) was not assigned precisely, due to its poor intensity, indicating that in CecXJ this part is rather rigid (or undergoes exchange phenomena). A22 and 25, identifying the inter-helix loop, are well visible together with signals from the C-terminus, thus confirming the flexibility of these elements, as previously observed in simulations [36].

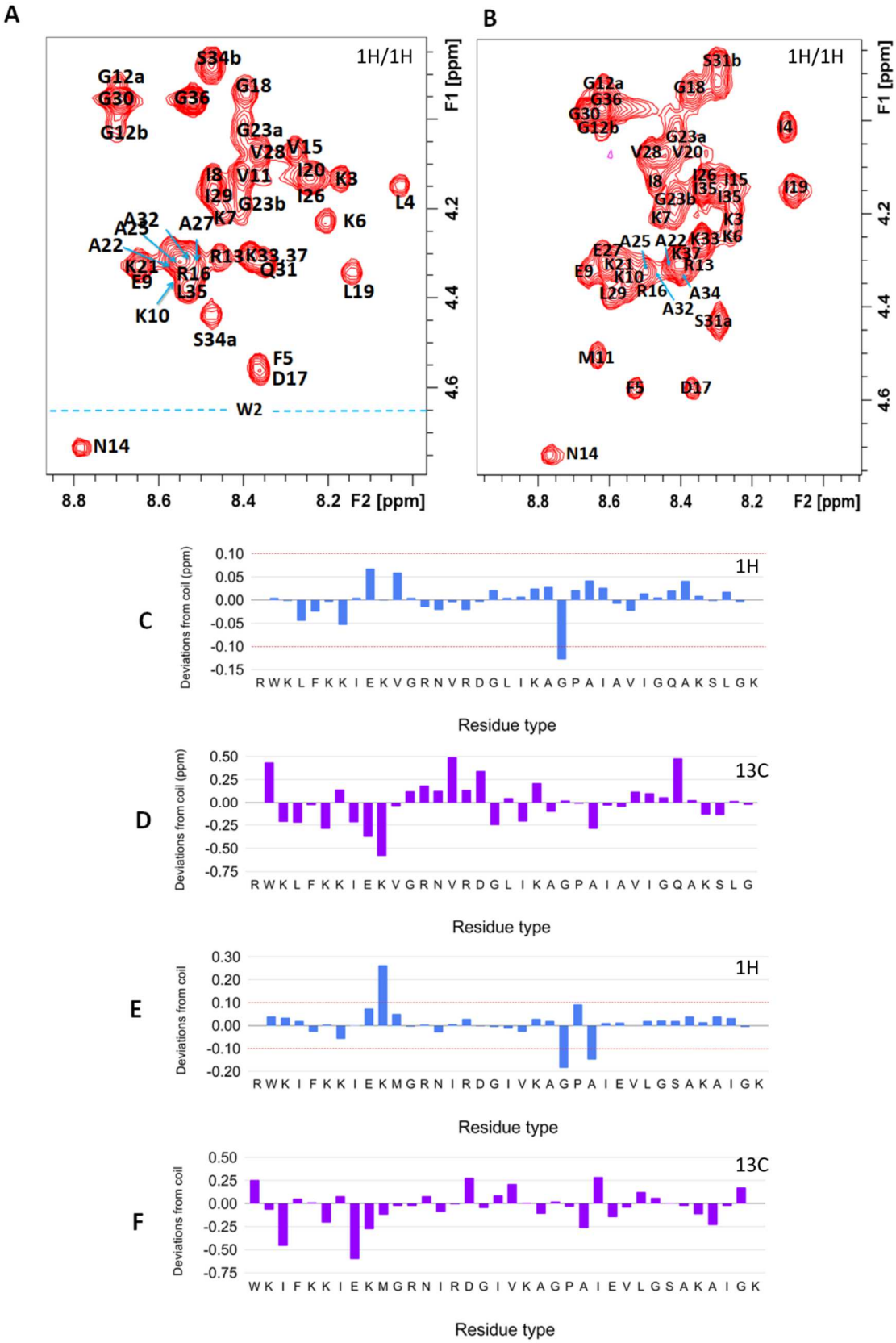

Figure 2. ***(A,B)*** *The ^{1}H assignment of CecA* ***(A)*** *and CecXJ* ***(B)*** *0.8 mM in 50 mM phosphate buffer at pH 6.6 and 278 K in the HN/H_{α} spectral region of $^{1}H,^{1}H$, TOCSY.* ***(C,D)*** *Chemical shift deviations from*

random coil values of H_α protons ***(C)*** *and C_α carbons* ***(D)*** *of CecA in solution.* ***(E,F)*** *Chemical shift deviations from random coil values of H_α protons* ***(E)*** *and C_α carbons* ***(F)*** *of CecXJ in solution.*

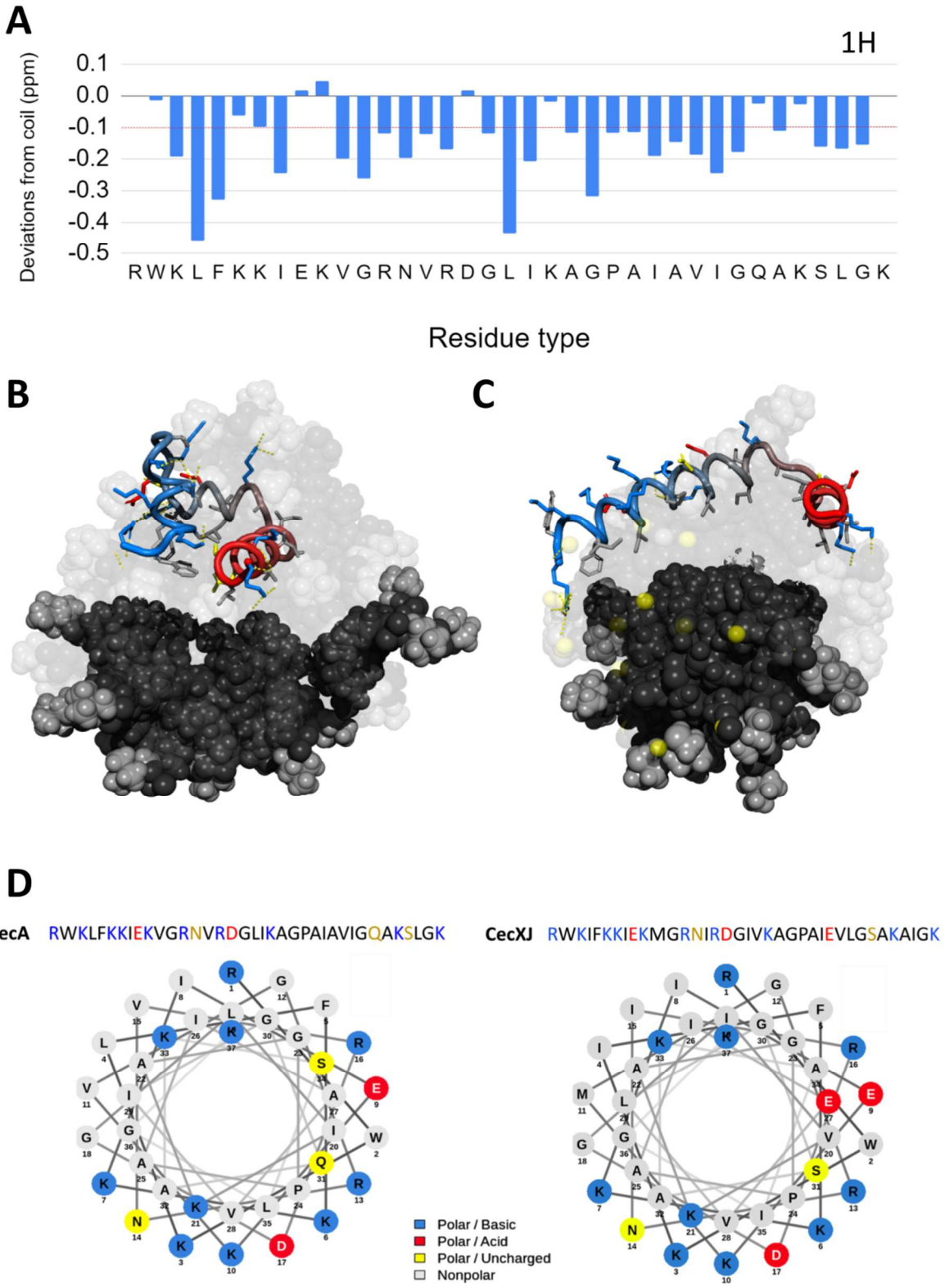

Figure 3. ***(A)*** *Chemical shift deviations from random coil values of H_α protons of CecA in the presence of DPC micelles, indicating the presence of alpha helical conformation.* ***(B,C)*** *MD snapshot of CecA*

(B) *and CecXJ* ***(C)*** *interacting with DPC micelles. Color code: phosphorus atom: yellow. DPC black (body) and light gray (choline group). For clarity, DPC molecules close to the peptides are shown as transparent spheres. BLP-3 is shown as a "tube" representation colored from blue (N-terminus) to red (C-terminus). Side chains are shown as sticks with the following color code: positively charged (blue), negatively charged (red), nonpolar (light gray), and polar (yellow).* ***(D)*** *Helical-wheel projections representing alpha-helix structures of CecA (left) and CecXJ (right). Hydrophobic amino acids are shown in gray, positively charged in blue, negatively charged in red and polar in yellow. Diagrams were created with NetWheels [61].*

3.3.3. Implication of the presence of three helices for CecA in DPC micelles

Despite the limitations in the use of DPC micelles as models for biological membranes [62,63], our data confirm that the substitution of M11 with beta-branched V11 creates a substantial difference in the secondary structure of CecA when interacting with a lipidic environment. The high curvature of DPC micelles do not seem to affect the integrity of helix I in CecXJ (see Figure 3C), suggesting that the effect observed for CecA is meaningful. The quality of spectra prevents an analysis in a more realistic membrane model suitable for liquid state NMR (e.g. isotropic bicelles) [62,63], unless isotopic labeling is performed. For this reason, in section 3.4 we relied on molecular dynamic simulations for a deeper understanding of how the flexibility observed in the presence of micelles might still be relevant in more realistic quasi-planar surfaces exposing headgroups representative of different cell types.

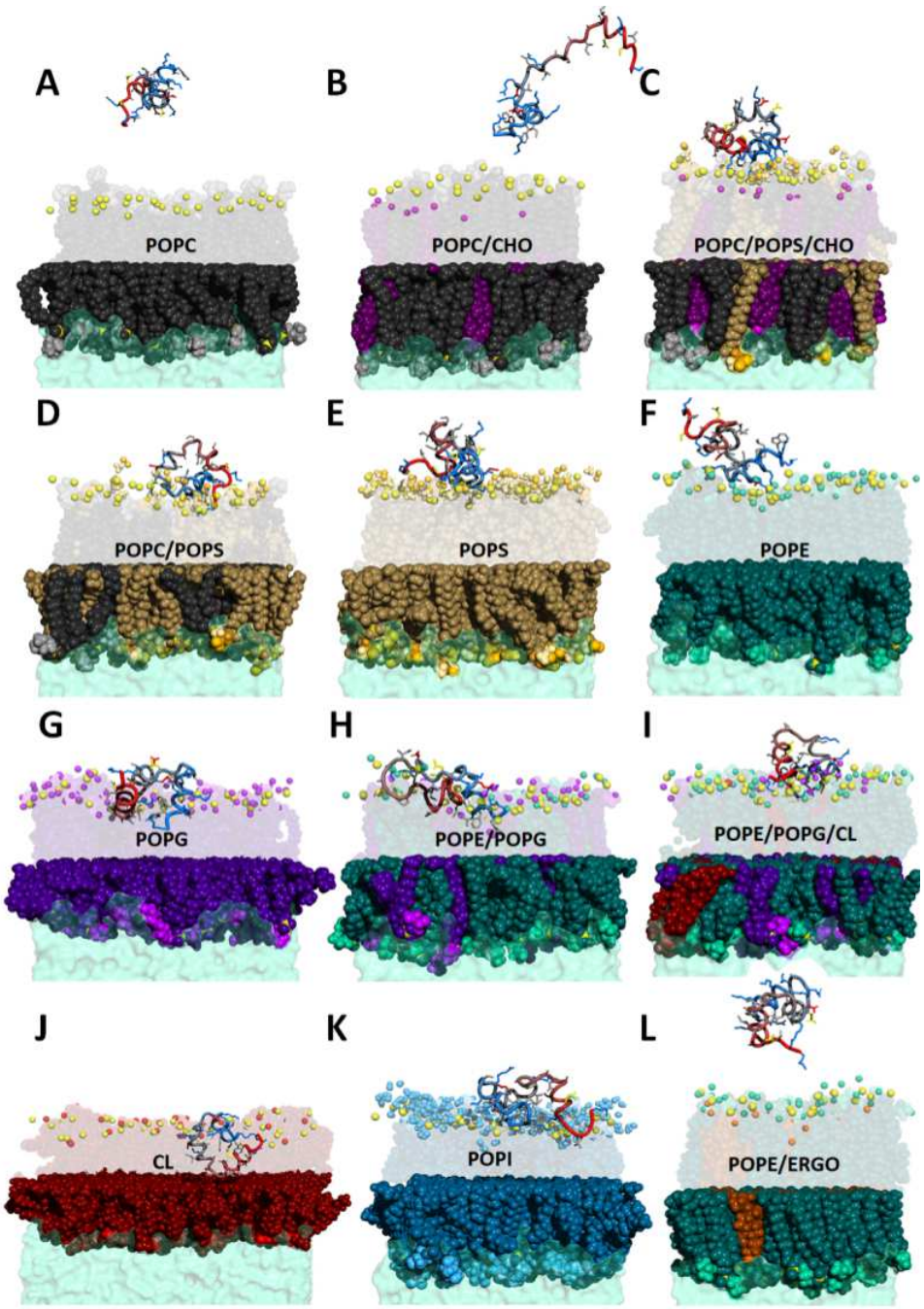

Figure 4. *Representative MD snapshots of CecA interacting with several membranes of variable phospholipid compositions. (A) 1-palmitoyl-2-oleoyl-glycero-3-phosphocholine (POPC); (B) POPC/cholesterol (CHO); (C) POPC/1-palmitoyl-2-oleoyl-sn-glycero-3-phospho-L-serine (POPS)/CHO; (D) POPC/POPS; (E) POPS; (F) 1-palmitoyl-2-oleoyl-sn-glycero-3-phosphoethanolamine (POPE); (G) 1-palmitoyl-2-oleoyl-sn-glycero-3-phospho-(1'-rac-glycerol) (POPG); (H) POPE/POPG; (I) POPE/POPG/cardiolipin (CL); (J) CL; (K) 1-palmitoyl-2-oleoyl-sn-glycero-3-phosphoinositol (POPI); (L) POPE/ergosterol (ERGO). Color code: phosphorus atom: yellow; POPC black (body) and light gray (choline group); POPS brown (body), gold (headgroup), light*

yellow (amine of the headgroup) and orange (carboxyl of the headgroup); POPE dark green (body), turquoise (headgroup), light green (amine of the headgroup); POPG dark violet (body), violet (headgroup), light violet (hydroxyls of the headgroup); POPI blue (body), light blue (headgroup), cyan (hydroxyls of the headgroup); CL dark red (body) and light red (headgroup); ERGO dark orange (body) and light orange (hydroxyl); CHO purple (body) and light purple (hydroxyl). For clarity, only functional groups of headgroups are shown (spheres) in the upper leaflet. CecA peptide is shown as a "tube" colored from blue (N-terminus) to red (C-terminus). Side chains are shown as sticks with the following color code: positively charged (blue), negatively charged (red), non-polar (light gray), polar (yellow).

3.4. The interaction of CecA and CecXJ with biomimetic membranes as studied by MD simulations

With the aim of characterizing the specific interactions at the basis of the biological activity of CecA, we have performed several MD simulations with biomimetic bilayers and compared them with our previous studies on CecXJ [36]. The study of long processes [64,65] such as the internalization of peptides into membrane bilayers is generally addressed by advanced sampling algorithms such as metadynamics, coarse-grain simulations, steered MD, umbrella-sampling, replica exchange or others [64,65]. In this work we want to unravel the initial steps characterizing the recognition of specific membranes, which explain the selectivity of cecropins for cancer and bacterial cells. In many cases our simulations are long enough to observe complete internalization, supporting their reported fast killing properties.

3.4.1. The interaction of CecA with mammalian biomimetic membranes

MD simulations do not show a relevant interaction between CecA and POPC membranes (Figure 4A), representing a simplified model of the external leaflet of mammalian cell membranes [66]. Polar and apolar contacts were calculated as the maximum of the radial distribution function [41] of CecA atoms from each phospholipid atom in the range of interatomic interaction distances (H-bonds, salt bridges and van der Waals). Only few interactions are established (Figure S7) and no peptide insertion is

observed (Figure S10). The addition of cholesterol (Figure 4B) does not change the overall behaviour, also in this case few polar (Figure S8) and apolar contacts are observed (Figure S11). These results are consistent with the reported lack of cytotoxicity for this peptide [28].

3.4.2. The interaction of CecA with cancerous biomimetic membranes

Cancer cells tend to expose PS and PE phospholipids in the outer leaflet of their membrane, while in non-cancerous cells they are both preferentially kept in the inner leaflet [10,11,67,68]. While exposure of PS introduces a net negative charge on the surface, PE displays a rather small headgroup which might facilitate the entrance of exogenous molecules, provided their chemical moieties are capable to break or replace the rich network of interaction among the PE amine and unesterified phosphate oxygen atoms.

Indeed, CecA appears to interact strongly with POPS containing membranes (Figure 4C-E), as indicated by the large variation in the order parameter observed in simulations with multiple peptides (Figure S13). Such a parameter expresses the degree of order of selected molecular fragments (the C-H moiety of the palmytoil chain in the present case) [69]. It can be used to monitor the perturbation in the organization of the membrane inner core caused by the presence of the peptide. Peptides which penetrate deeply in membrane bilayers generally lower the value of such parameters; however, a strong superficial interaction can in some cases increase the lipid packing with consequent increase of the order parameter [36,70–72]. In any case, a significant perturbation of its value indicates a strong interaction.

Multiple polar contacts are established between R and K residues and the carboxyl of serine headgroup (and to a minor extent with the phosphate moiety), thus testifying the specificity of CecA for PS phospholipids (Figure S7). Additionally, E9 side chain sporadically interacts with PS amine. Such contacts are maintained when the ratio of POPS is lowered to 50% (i.e., POPC/POPS (50/50%)) or even to 35% and cholesterol is added (POPC/POPS/CHO (35/35/30%)) (Figure S9). The latter more complex models aim at mimicking more realistic cancer membrane compositions, including the effect of cholesterol on fluidity [73].

Despite the strong affinity for PS-containing membranes, poor penetration is observed, as demonstrated by the low occurrence of apolar contacts (Figures S10, S12). As in the case of CecXJ [36], we believe that CecA might act as a cell penetrating peptide (CPP) and translocates by induction

of endocytosis or by means of flip-flop equilibria once tightly bound to the membrane surface, as hypothesized for peptides rich on Arginines or Leucines [17–20].

When evaluating the interaction of CecA with PE (Figure 4F), we found much less polar contacts than in the case of PS (Figure S7) and rare apolar contacts (Figure S10). This is consistent with the low affinity for uncharged membranes, as it was the case for PC. Nonetheless, sparse apolar contacts can be observed (Figure S10), indicating some degree of penetration (probably due to the accessibility provided by the small head group of PE) that can also be monitored by a perturbation of the order parameter of the lipid acyl chains (Figures S13,S14). As in the previous case, CecA interacts by means of helix I, forming salt bridges between the R and K side chains with oxygen atom of the phosphate groups but also between the carboxylate of E and D residues with the amine of the ethanolamine headgroup (Figure S7).

Overall, CecA displays a much higher affinity for POPS than POPE. This is also reflected by the important invagination of PS membranes in the presence of CecA, that can be monitored as an increase and decrease of the area per lipid in the inner (distal) and outer (proximal) leaflets, respectively (Figure S15). These findings suggest that if its anticancer activity is due to the interaction with a phospholipid, PS is more likely to be directly involved.

3.4.3. The interaction of CecA with mitochondrial biomimetic membranes

Cardiolipin is the most characteristic lipid in mitochondria [24], making up to 25% of the inner membrane of such organelle, also rich in PE [74]. CecXJ has been shown to induce apoptosis in cancer cells [75], probably due to its ability to interact with CL phospholipid [36]. In cancer cells, mitochondria often express a higher amount of CL in the outer membrane than in non-cancerous cells [76].

CecA acts very similarly to CecXJ in our simulations, in that we observe a marked preference for CL (Figure 4J). Part of the reason resides in the strong electrostatic attractions (CL displays a doubly negative charge while CecA has an overall +8 charge). However, differences exist in the mode of interaction: while CecXJ tends to penetrate by means of helix I [36], CecA also uses helix II (Figures S8, S11). This is probably due to the E27A mutation in helix II which removes local electrostatic repulsion with the surface. The accessibility of CL bilayers, characterized by the absence

of a headgroup must also play a role because such helix penetrates CL-free bilayers with much lower frequencies (Figures S10-S12).

3.4.4. The interaction of CecA with bacterial biomimetic membranes

Phosphatidylglycerol (PG) is hardly found in eukaryotes and can be considered as a signature of bacterial membranes [66,77,78]. In bacteria, PG is almost invariably associated with PE and, depending on the bacterial species, with CL [77,78].

Simulations with pure POPG membranes (Figure 4G) predict an affinity comparable to that observed with POPS, as suggested by frequent polar contacts in which K and R side chains form salt-bridges with phosphate oxygen atoms (Figure S7). The absence of polar contact with hydroxyl moieties of the PG headgroup testify a somewhat deeper insertion than in the case of PS. Accordingly, many apolar contacts are formed between the side chains of CecA and the acyl chains of POPG, reaching the inner core of the bilayer (Figure S10). Also the impacts on the order parameter (Figures S13,S14) and the area per lipid (Figure S14) are of similar importance as in the case of PS. Despite all these similarities, simulations indicate that CecA is able to penetrate POPG membranes deeply, while it strongly attaches to the surface of POPS membranes, suggesting a different mechanism of action.

In more realistic bacterial membranes, where PE and PG co-exist [78] (Figure 4H), a clear preference is apparent for PG (Figure S8), probably due to its negative charge (PE is neutral), which attracts this extremely positive peptide. The high occurrence of apolar contacts reveal that CecA penetrates deeply as in the case of pure PG (Figure S10), even reaching the terminal part of the lipid acyl chains (Figure S11).

For a more complete analysis we also examined the case of membranes composed of PE, PG and CL, often found in bacteria [78] (Figure 4I). The analysis of the polar contacts clearly shows a preference for the latter (Figure S8). As in the case of pure CL membranes (see section 3.3.3), we observe a deep insertion of helix II (Figure S11), probably due to the increased negative charge, and augmented accessibility [78] caused by the presence of CL.

3.4.5. The interaction of CecA with fungal biomimetic membranes

CecA has been shown to display antifungal activity [33,34]. Fungal membranes are mainly composed of PE, but they can also contain PS and PI [79–81]. This is the case of *Beauveria bassiana*, one of the targets of CecA, that can also expose PG under certain environmental conditions [79,80,82]. Ergosterol (ERGO) is the sterol characterizing the fungal kingdom and the main target of many antifungal compounds [83].

The introduction of ERGO in POPE membranes does not modify what we had previously observed with pure POPE membranes (Figure 4L). Polar contacts are sparse and mostly established with helix I (Figure S8). The penetration of the peptide is poor (Figure S11) even though it can affect the order parameter of acyl chains (Figures S13, S14).

On the contrary, CecA interacts significantly with POPI membranes (Figure 4K) making salt bridges with their phosphate moieties by means of lysine and arginine side chains. Few H-bonds can be formed also with the inositol hydroxyl groups by means of S34 (Figure S7). Residues able to establish polar contacts with the membrane are often flanked by hydrophobic residues able to penetrate deeply in the bilayer. We have observed this pattern often [36,70], especially in flexible regions. For example, the N-terminal amine, which is capable of forming strong polar contacts is often followed by an apolar residue [36,84] which inserts its side chain in the target bilayer. In the case of CecA, the couple S34 and L35 could act similarly, as indicated by the deep insertion of the latter in POPI bilayers (Figure S10).

In summary, the antifungal activity of CecA could be due to a direct interaction with PI rather than PE, although it should be considered that also PS can be present in some fungi and play a role.

4. Conclusions

CecXJ and CecA are among the very few peptides active against esophageal cancer cells. They are highly sequence homologous and share several similarities in terms of both anticancer and antimicrobial activity. Nonetheless, CecA displays a somewhat higher anticancer activity [27,28], suggesting that the comparison of their sequence might reveal key amino acids for the development of new anticancer agents for the treatment of esophageal cancer. The picture coming out from NMR and MD results show how both CecXJ and CecA get structured upon interaction with their target membranes. While a strong superficial binding is observed with membranes mimicking the external

leaflet of cancer cells (exposing PS), both peptides destabilize the inner core of bilayers mimicking mitochondria. These findings are in agreement with the reported cell penetrating and apoptotic properties, where strong superficial binding (followed by internalization by endocitosis of flip-flop mechanisms) allows the entrance of the peptide in the cytoplasm and damage to mitochondrial membranes triggers apoptosis. The same mechanism can also explain the antibacterial activity of these compounds, in light of the similarity of mitochondrial and bacterial bilayers. Our data also show that the enhanced anticancer activity of CecA might stem from the substitution of E27 with the non-charged residue A27 and the replacement of M11 with the beta branched V11. The former facilitates the interaction of helix II with negatively charged surfaces (as those found in mitochondria), which adds up to the strong binding of helix I. The latter is able to break helix I into two helices, allowing CecA to adapt and penetrate more easily in mitochondrial, bacterial and fungal membranes.

ASSOCIATED CONTENT

Author Contributions

Conceptualization, Francisco Ramos-Martín and Nicola D'Amelio; Data curation, Nicola D'Amelio; Formal analysis, Francisco Ramos-Martín, Claudia Herrera-León and Nicola D'Amelio; Funding acquisition, Nicola D'Amelio; Investigation, Francisco Ramos-Martín and Claudia Herrera-León ; Methodology, Francisco Ramos-Martín and Nicola D'Amelio; Project administration, Nicola D'Amelio; Software, Francisco Ramos-Martín and Nicola D'Amelio; Supervision, Nicola D'Amelio;Writing – original draft, Francisco Ramos-Martín, Claudia Herrera-Léon and Nicola D'Amelio; Writing – review & editing, Francisco Ramos-Martín, Claudia Herrera-León, and Nicola D'Amelio. All authors have given approval to the final version of the manuscript.

Funding sources

Francisco Ramos-Martín's PhD scholarship was co-funded by Conseil régional des Hauts-de-France and by European Fund for Economic and Regional Development (FEDER); Claudia Herrera-León's PhD scholarship was funded by the National Council for Science and Technology (CONACYT). This work was partly supported through the ANR Natural-Arsenal project.

Acknowledgements

We thank the Matrics platform at the University “Picardie Jules Verne” and the “Méso-centre de Calcul Scientifique Intensif” at the University of Lille for providing computing resources. We thank Olivia Auvy and Matthieu Magdziak for contributing to the NMR assignment of CecA and CecXJ.

REFERENCES

[1] F.R. Talukdar, M. di Pietro, M. Secrier, M. Moehler, K. Goepfert, S.S.C. Lima, L.F.R. Pinto, D. Hendricks, M.I. Parker, Z. Herceg, Molecular landscape of esophageal cancer: implications for early detection and personalized therapy, Ann. N. Y. Acad. Sci. 1434 (2018) 342–359.
[2] E.O. Then, M. Lopez, S. Saleem, V. Gayam, T. Sunkara, A. Culliford, V. Gaduputi, Esophageal Cancer: An Updated Surveillance Epidemiology and End Results Database Analysis, World J. Oncol. 11 (2020) 55–64.
[3] L.E. Papanicolas, D.L. Gordon, S.L. Wesselingh, G.B. Rogers, Not Just Antibiotics: Is Cancer Chemotherapy Driving Antimicrobial Resistance?, Trends Microbiol. 26 (2018) 393–400.
[4] W. Yang, J. Ma, W. Zhou, X. Zhou, B. Cao, H. Zhang, Q. Zhao, D. Fan, L. Hong, Molecular mechanisms and clinical implications of miRNAs in drug resistance of esophageal cancer, Expert Rev. Gastroenterol. Hepatol. 11 (2017). https://doi.org/10.1080/17474124.2017.1372189.
[5] Q.-X. Teng, X. Luo, Z.-N. Lei, J.-Q. Wang, J. Wurpel, Z. Qin, D.-H. Yang, The Multidrug Resistance-Reversing Activity of a Novel Antimicrobial Peptide, Cancers . 12 (2020) 1963.
[6] V.E. Wang, J.R. Grandis, A.H. Ko, New Strategies in Esophageal Carcinoma: Translational Insights from Signaling Pathways and Immune Checkpoints, Clin. Cancer Res. 22 (2016) 4283–4290.
[7] C. Pericay, I. Macías-Declara, V. Arrazubi, L. Vilà, M. Marín, Treatment in esophagogastric junction cancer: Past, present and future, Cir. Esp. 97 (2019) 459–464.
[8] L. Sanz Álvarez, E. Turienzo Santos, J.L. Rodicio Miravalles, M. Moreno Gijón, S. Amoza Pais, S. Sanz Navarro, A. Rizzo Ramos, Evidence in follow-up and prognosis of esophagogastric junction cancer, Cir. Esp. 97 (2019) 465–469.
[9] M. Kalmouni, S. Al-Hosani, M. Magzoub, Cancer targeting peptides, Cell. Mol. Life Sci. 76 (2019). https://doi.org/10.1007/s00018-019-03061-0.
[10] E.M. Bevers, P.L. Williamson, Getting to the Outer Leaflet: Physiology of Phosphatidylserine Exposure at the Plasma Membrane, Physiol. Rev. 96 (2016) 605–645.
[11] T.E. Merchant, P.W. de Graaf, B.D. Minsky, H. Obertop, T. Glonek, Esophageal cancer phospholipid characterization by 31P NMR, NMR Biomed. 6 (1993) 187–193.
[12] R. Liu, Y. Peng, X. Li, Y. Wang, E. Pan, W. Guo, Y. Pu, L. Yin, Identification of plasma metabolomic profiling for diagnosis of esophageal squamous-cell carcinoma using an UPLC/TOF/MS platform, Int. J. Mol. Sci. 14 (2013) 8899–8911.
[13] D. Wu, Y. Gao, Y. Qi, L. Chen, Y. Ma, Y. Li, Peptide-based cancer therapy: opportunity and challenge, Cancer Lett. 351 (2014). https://doi.org/10.1016/j.canlet.2014.05.002.
[14] G. Yu, D.Y. Baeder, R.R. Regoes, J. Rolff, Predicting drug resistance evolution: insights from antimicrobial peptides and antibiotics, Proc. Biol. Sci. 285 (2018). https://doi.org/10.1098/rspb.2017.2687.
[15] B. Kintses, O. Méhi, E. Ari, M. Számel, Á. Györkei, P.K. Jangir, I. Nagy, F. Pál, G. Fekete, R. Tengölics, Á. Nyerges, I. Likó, A. Bálint, T. Molnár, B. Bálint, B.M. Vásárhelyi, M. Bustamante, B. Papp, C. Pál, Phylogenetic barriers to horizontal transfer of antimicrobial peptide resistance genes in the human gut microbiota, Nat Microbiol. 4 (2019) 447–458.
[16] L. Xia, Y. Wu, J.I. Ma, J. Yang, F. Zhang, The antibacterial peptide from cecropinXJ induced growth arrest and apoptosis in human hepatocellular carcinoma cells, Oncol. Lett. 12 (2016) 57–62.
[17] T. Fuselier, W.C. Wimley, Spontaneous Membrane Translocating Peptides: The Role of Leucine-Arginine Consensus Motifs, Biophys. J. 113 (2017) 835–846.
[18] Y. Su, T. Doherty, A.J. Waring, P. Ruchala, M. Hong, Roles of arginine and lysine residues in the translocation of a cell-penetrating peptide from (13)C, (31)P, and (19)F solid-state NMR, Biochemistry. 48 (2009). https://doi.org/10.1021/bi900080d.
[19] H.L. Amand, K. Fant, B. Nordén, E.K. Esbjörner, Stimulated endocytosis in penetratin uptake: effect of arginine and lysine, Biochem. Biophys. Res. Commun. 371 (2008) 621–625.
[20] A. Rice, J. Wereszczynski, Probing the disparate effects of arginine and lysine residues on antimicrobial peptide/bilayer association, Biochim. Biophys. Acta Biomembr. 1859 (2017) 1941–1950.

[21] S.B. Fonseca, M.P. Pereira, R. Mourtada, M. Gronda, K.L. Horton, R. Hurren, M.D. Minden, A.D. Schimmer, S.O. Kelley, Rerouting chlorambucil to mitochondria combats drug deactivation and resistance in cancer cells, Chem. Biol. 18 (2011) 445–453.
[22] S.R. Jean, M.P. Pereira, S.O. Kelley, Structural modifications of mitochondria-targeted chlorambucil alter cell death mechanism but preserve MDR evasion, Mol. Pharm. 11 (2014) 2675–2682.
[23] S.B. Fonseca, S.O. Kelley, Peptide-chlorambucil conjugates combat pgp-dependent drug efflux, ACS Med. Chem. Lett. 2 (2011) 419–423.
[24] D. Casares, P.V. Escribá, C.A. Rosselló, Membrane Lipid Composition: Effect on Membrane and Organelle Structure, Function and Compartmentalization and Therapeutic Avenues, Int. J. Mol. Sci. 20 (2019). https://doi.org/10.3390/ijms20092167.
[25] E.K. Lei, M.P. Pereira, S.O. Kelley, Tuning the intracellular bacterial targeting of peptidic vectors, Angew. Chem. Int. Ed Engl. 52 (2013) 9660–9663.
[26] L. Xia, Y. Wu, S. Kang, J. Ma, J. Yang, F. Zhang, CecropinXJ, a silkworm antimicrobial peptide, induces cytoskeleton disruption in esophageal carcinoma cells, Acta Biochim. Biophys. Sin. . 46 (2014) 867–876.
[27] L.-J. Xia, Y.-L. Wu, J. Ma, F.-C. Zhang, Therapeutic effects of antimicrobial peptide on malignant ascites in a mouse model, Mol. Med. Rep. 17 (2018) 6245–6252.
[28] P. Xu, D. Lv, X. Wang, Y. Wang, C. Hou, K. Gao, X. Guo, Inhibitory effects of Bombyx mori antimicrobial peptide cecropins on esophageal cancer cells, Eur. J. Pharmacol. 887 (2020) 173434.
[29] M. Sang, J. Zhang, Q. Zhuge, Selective cytotoxicity of the antibacterial peptide ABP-dHC-Cecropin A and its analog towards leukemia cells, Eur. J. Pharmacol. 803 (2017) 138–147.
[30] E. Lee, A. Shin, Y. Kim, Anti-inflammatory activities of cecropin A and its mechanism of action, Arch. Insect Biochem. Physiol. 88 (2015). https://doi.org/10.1002/arch.21193.
[31] J. Zhang, A. Movahedi, X. Wang, X. Wu, T. Yin, Q. Zhuge, Molecular structure, chemical synthesis, and antibacterial activity of ABP-dHC-cecropin A from drury (Hyphantria cunea), Peptides. 68 (2015) 197–204.
[32] M.B. Tincho, T. Morris, M. Meyer, A. Pretorius, Antibacterial Activity of Rationally Designed Antimicrobial Peptides, Int. J. Microbiol. 2020 (2020). https://doi.org/10.1155/2020/2131535.
[33] S.J. Islam, S. Bezbaruah, J. Kalita, A Review on Antimicrobial Peptides from Bombyx mori L and Their Application in Plant and Animal Disease Control, Journal of Advances in Biology & Biotechnology. (2016) 1–15.
[34] Dingding Lu, Tao Geng, Chengxiang Hou, Yuxia Huang, Guangxing Qin, Xijie Guo, Bombyx mori cecropin A has a high antifungal activity to entomopathogenic fungus Beauveria bassiana, Gene. 583 (2016) 29–35.
[35] J.M. Cerón, J. Contreras-Moreno, E. Puertollano, G.Á. de Cienfuegos, M.A. Puertollano, M.A. de Pablo, The antimicrobial peptide cecropin A induces caspase-independent cell death in human promyelocytic leukemia cells, Peptides. 31 (2010) 1494–1503.
[36] F. Ramos-Martín, N. D'Amelio, Molecular Basis of the Anticancer and Antibacterial Properties of CecropinXJ Peptide: An In Silico Study, Int. J. Mol. Sci. 22 (2021) 691.
[37] S. Jo, T. Kim, W. Im, Automated builder and database of protein/membrane complexes for molecular dynamics simulations, PLoS One. 2 (2007) e880.
[38] A. Lamiable, P. Thévenet, J. Rey, M. Vavrusa, P. Derreumaux, P. Tufféry, PEP-FOLD3: faster de novo structure prediction for linear peptides in solution and in complex, Nucleic Acids Res. 44 (2016) W449–54.
[39] M.J. Abraham, T. Murtola, R. Schulz, S. Páll, J.C. Smith, B. Hess, E. Lindahl, GROMACS: High performance molecular simulations through multi-level parallelism from laptops to supercomputers, SoftwareX. 1-2 (2015) 19–25. https://doi.org/10.1016/j.softx.2015.06.001.
[40] J. Huang, S. Rauscher, G. Nawrocki, T. Ran, M. Feig, B.L. de Groot, H. Grubmüller, A.D. MacKerell, CHARMM36m: an improved force field for folded and intrinsically disordered proteins, Nat. Methods. 14 (2016) 71–73.
[41] H.J.C. Berendsen, J.P.M. Postma, W.F. van Gunsteren, J. Hermans, Interaction Models for Water in Relation to Protein Hydration, The Jerusalem Symposia on Quantum Chemistry and Biochemistry. (1981) 331–342. https://doi.org/10.1007/978-94-015-7658-1_21.
[42] H.J.C. Berendsen, J.P.M. Postma, W.F. van Gunsteren, A. DiNola, J.R. Haak, Molecular dynamics with coupling to an external bath, The Journal of Chemical Physics. 81 (1984) 3684–3690. https://doi.org/10.1063/1.448118.
[43] M. Parrinello, A. Rahman, Polymorphic transitions in single crystals: A new molecular dynamics method, Journal of Applied Physics. 52 (1981) 7182–7190. https://doi.org/10.1063/1.328693.

[44] S. Nosé, A unified formulation of the constant temperature molecular dynamics methods, The Journal of Chemical Physics. 81 (1984) 511–519. https://doi.org/10.1063/1.447334.
[45] W.G. Hoover, Canonical dynamics: Equilibrium phase-space distributions, Phys. Rev. A Gen. Phys. 31 (1985) 1695–1697.
[46] S. Buchoux, FATSLiM: a fast and robust software to analyze MD simulations of membranes, Bioinformatics. 33 (2017) 133–134.
[47] W.L. DeLano, Pymol: An open-source molecular graphics tool, CCP4 Newsletter on Protein Crystallography. 40 (2002) 82–92.
[48] J.T. Nielsen, F.A.A. Mulder, POTENCI: prediction of temperature, neighbor and pH-corrected chemical shifts for intrinsically disordered proteins, J. Biomol. NMR. 70 (2018) 141–165.
[49] M.-A. Sani, F. Separovic, How Membrane-Active Peptides Get into Lipid Membranes, Acc. Chem. Res. 49 (2016) 1130–1138.
[50] J. Lei, L. Sun, S. Huang, C. Zhu, P. Li, J. He, V. Mackey, D.H. Coy, Q. He, The antimicrobial peptides and their potential clinical applications, Am. J. Transl. Res. 11 (2019). https://pubmed.ncbi.nlm.nih.gov/31396309/ (accessed November 9, 2021).
[51] J. Wang, X. Dou, J. Song, Y. Lyu, X. Zhu, L. Xu, W. Li, A. Shan, Antimicrobial peptides: Promising alternatives in the post feeding antibiotic era, Med. Res. Rev. 39 (2019) 831–859.
[52] Y.-B. Huang, L.-Y. He, H.-Y. Jiang, Y.-X. Chen, Role of helicity on the anticancer mechanism of action of cationic-helical peptides, Int. J. Mol. Sci. 13 (2012) 6849–6862.
[53] P.Y. Chou, G.D. Fasman, Prediction of the secondary structure of proteins from their amino acid sequence, Adv. Enzymol. Relat. Areas Mol. Biol. 47 (1978). https://doi.org/10.1002/9780470122921.ch2.
[54] T.P. Creamer, G.D. Rose, Side-chain entropy opposes alpha-helix formation but rationalizes experimentally determined helix-forming propensities, Proc. Natl. Acad. Sci. U. S. A. 89 (1992) 5937–5941.
[55] R. Lohia, R. Salari, G. Brannigan, Sequence specificity despite intrinsic disorder: How a disease-associated Val/Met polymorphism rearranges tertiary interactions in a long disordered protein, PLoS Comput. Biol. 15 (2019) e1007390.
[56] W. Kabsch, C. Sander, Dictionary of protein secondary structure: pattern recognition of hydrogen-bonded and geometrical features, Biopolymers. 22 (1983) 2577–2637.
[57] F. Ramos-Martín, T. Annaval, S. Buchoux, C. Sarazin, N. D'Amelio, ADAPTABLE: a comprehensive web platform of antimicrobial peptides tailored to the user's research, Life Sci Alliance. 2 (2019). https://doi.org/10.26508/lsa.201900512.
[58] D. Liu, J. Liu, J. Li, L. Xia, J. Yang, S. Sun, J. Ma, F. Zhang, A potential food biopreservative, CecXJ-37N, non-covalently intercalates into the nucleotides of bacterial genomic DNA beyond membrane attack, Food Chem. 217 (2017) 576–584.
[59] Y. Wang, O. Jardetzky, Probability-based protein secondary structure identification using combined NMR chemical-shift data, Protein Sci. 11 (2002) 852–861.
[60] D.S. Wishart, Interpreting protein chemical shift data, Prog. Nucl. Magn. Reson. Spectrosc. 58 (2011) 62–87.
[61] A.R. Mól, M.S. Castro, W. Fontes, NetWheels: A web application to create high quality peptide helical wheel and net projections, bioRxiv. (2018). https://doi.org/10.1101/416347.
[62] D.E. Warschawski, A.A. Arnold, M. Beaugrand, A. Gravel, É. Chartrand, I. Marcotte, Choosing membrane mimetics for NMR structural studies of transmembrane proteins, Biochim. Biophys. Acta. 1808 (2011) 1957–1974.
[63] F. Porcelli, A. Ramamoorthy, G. Barany, G. Veglia, On the Role of NMR Spectroscopy for Characterization of Antimicrobial Peptides, Membrane Proteins. (2013) 159–180. https://doi.org/10.1007/978-1-62703-583-5_9.
[64] F.G. Avci, B.S. Akbulut, E. Ozkirimli, Membrane Active Peptides and Their Biophysical Characterization, Biomolecules. 8 (2018). https://doi.org/10.3390/biom8030077.
[65] S.J. Marrink, V. Corradi, P.C.T. Souza, H.I. Ingólfsson, D.P. Tieleman, M.S.P. Sansom, Computational Modeling of Realistic Cell Membranes, Chem. Rev. 119 (2019) 6184–6226.
[66] A. Zachowski, Phospholipids in animal eukaryotic membranes: transverse asymmetry and movement, Biochem. J. 294 (Pt 1) (1993) 1–14.
[67] K. Emoto, N. Toyama-Sorimachi, H. Karasuyama, K. Inoue, M. Umeda, Exposure of phosphatidylethanolamine on the surface of apoptotic cells, Exp. Cell Res. 232 (1997) 430–434.
[68] D.A. Phoenix, F. Harris, M. Mura, S.R. Dennison, The increasing role of phosphatidylethanolamine as a lipid receptor in the action of host defence peptides, Prog. Lipid Res. 59 (2015) 26–37.
[69] C. Aisenbrey, A. Marquette, B. Bechinger, The Mechanisms of Action of Cationic Antimicrobial

Peptides Refined by Novel Concepts from Biophysical Investigations, Adv. Exp. Med. Biol. 1117 (2019) 33–64.
[70] F. Ramos-Martín, C. Herrera-León, V. Antonietti, P. Sonnet, C. Sarazin, N. D'Amelio, Antimicrobial Peptide K11 Selectively Recognizes Bacterial Biomimetic Membranes and Acts by Twisting Their Bilayers, Pharmaceuticals . 14 (2020). https://doi.org/10.3390/ph14010001.
[71] K.A. Henzler-Wildman, G.V. Martinez, M.F. Brown, A. Ramamoorthy, Perturbation of the hydrophobic core of lipid bilayers by the human antimicrobial peptide LL-37, Biochemistry. 43 (2004) 8459–8469.
[72] E.J. Dufourc, I.C. Smith, J. Dufourcq, Molecular details of melittin-induced lysis of phospholipid membranes as revealed by deuterium and phosphorus NMR, Biochemistry. 25 (1986) 6448–6455.
[73] P.M.R. Cruz, H. Mo, W.J. McConathy, N. Sabnis, A.G. Lacko, The role of cholesterol metabolism and cholesterol transport in carcinogenesis: a review of scientific findings, relevant to future cancer therapeutics, Front. Pharmacol. 4 (2013) 119.
[74] N. Lane, W. Martin, The energetics of genome complexity, Nature. 467 (2010) 929–934.
[75] Y.-L. Wu, L.-J. Xia, J.-Y. Li, F.-C. Zhang, CecropinXJ inhibits the proliferation of human gastric cancer BGC823 cells and induces cell death in vitro and in vivo, Int. J. Oncol. 46 (2015) 2181–2193.
[76] C.M. Julienne, M. Tardieu, S. Chevalier, M. Pinault, P. Bougnoux, F. Labarthe, C. Couet, S. Servais, J.F. Dumas, Cardiolipin content is involved in liver mitochondrial energy wasting associated with cancer-induced cachexia without the involvement of adenine nucleotide translocase, Biochim. Biophys. Acta. 1842 (2014). https://doi.org/10.1016/j.bbadis.2014.02.003.
[77] R.M. Epand, R.F. Epand, Lipid domains in bacterial membranes and the action of antimicrobial agents, Biochim. Biophys. Acta. 1788 (2009) 289–294.
[78] S.C. Lopes, C.S. Neves, P. Eaton, P. Gameiro, Improved model systems for bacterial membranes from differing species: the importance of varying composition in PE/PG/cardiolipin ternary mixtures, Mol. Membr. Biol. 29 (2012) 207–217.
[79] H. Liu, X. Zhao, M. Guo, H. Liu, Z. Zheng, Growth and metabolism of Beauveria bassiana spores and mycelia, BMC Microbiol. 15 (2015) 267.
[80] Y. Zhang, M. Tang, Z. Dong, D. Zhao, L. An, H. Zhu, Q. Xia, P. Zhao, Synthesis, secretion, and antifungal mechanism of a phosphatidylethanolamine-binding protein from the silk gland of the silkworm Bombyx mori, Int. J. Biol. Macromol. 149 (2020) 1000–1007.
[81] J.D. Weete, Lipid Biochemistry of Fungi and Other Organisms, Springer Science & Business Media, 2012.
[82] F. Luo, Q. Wang, C. Yin, Y. Ge, F. Hu, B. Huang, H. Zhou, G. Bao, B. Wang, R. Lu, Z. Li, Differential metabolic responses of Beauveria bassiana cultured in pupae extracts, root exudates and its interactions with insect and plant, J. Invertebr. Pathol. 130 (2015) 154–164.
[83] A.M. Fuentefria, B. Pippi, D.F. Dalla Lana, K.K. Donato, S.F. de Andrade, Antifungals discovery: an insight into new strategies to combat antifungal resistance, Lett. Appl. Microbiol. 66 (2018) 2–13.
[84] T. Annaval, F. Ramos-Martín, C. Herrera-León, M. Adélaïde, V. Antonietti, S. Buchoux, P. Sonnet, C. Sarazin, N. D'Amelio, Antimicrobial bombinin-like peptide 3 selectively recognizes and inserts into bacterial biomimetic bilayers in multiple steps, J. Med. Chem. (2021). https://doi.org/10.1021/acs.jmedchem.1c00310.

Graphical Abstract

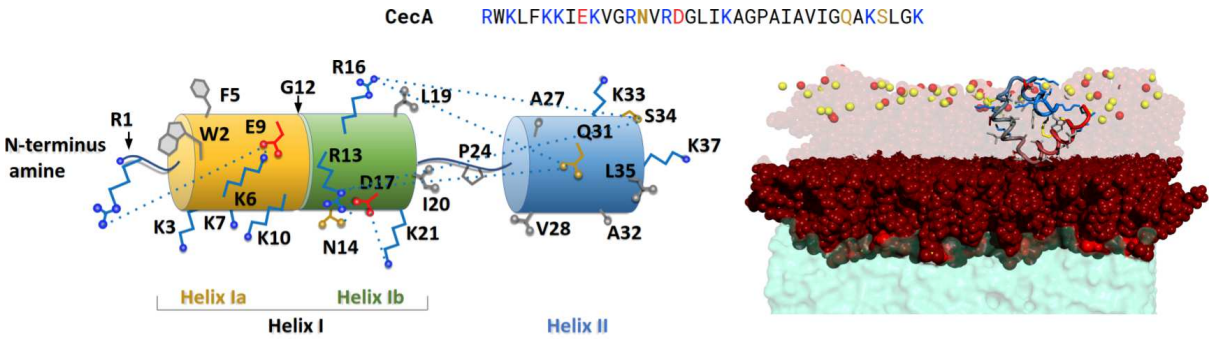

Three helix bundle formation upon membrane interaction